Transactions on Cancer (2023)
Clausius Scientific Press, Canada

DOI: 10.23977/tranc.2023.040114
ISSN 2523-6482 Vol. 4 Num. 1

Anticancer Activity of Polysaccharides from Castanea Mollissima Blume in H22 Tumor-Bearing Mice

Jinyan Xue, Yueying Wang, Chensa Zhang, Yulu Chang, Yuzi Wang, Liman Liang, Kui Niu*

School of Chemical Engineering, Hebei Normal University of Science and Technology, Qinhuangdao, Hebei, 066004, China
**Corresponding author*

Keywords: Chestnut polysaccharide, Anticancer activity, H22 tumor, Three phase partitioning

Abstract: In this study, chestnut polysaccharides (TCP) obtained through hot water extraction and purified using three-phase partitioning method were fed to H22 hepatoma-bearing mice to investigate their inhibitory effects on the solid tumors. It was shown that oral administration of TCP markedly suppressed the tumor growth and alleviated spleen enlargement and thymus atrophy. The tumor inhibition rates for the low-dose group [100 mg/(kg d)] and the high-dose group [500 mg/(kg d)] of TCP were 35.64% and 56.61%, respectively. TCP also remarkably enhanced the splenocyte proliferation induced by ConA or LPS in mice, notably improved the macrophage phagocytosis, and increased the percentages of $CD3^+$, $CD4^+$, and $CD8^+$ T lymphocytes in peripheral blood of mice. The research verifies that TCP demonstrates anti-tumor properties by amplifying the immune defense systems of the host, showcasing significant promise for applications in medicinal and functional food sectors.

1. Introduction

Chestnuts, scientifically known as *Castanea*, are among the prominent edible nuts renowned for their rich nutritional profile and multiple health benefits[1]. Native to temperate regions, chestnuts have been a staple in human diets for millennia, not just for their palatable taste but also for the plethora of nutrients they offer. Unlike other nuts, chestnuts are low in fat but are rich in carbohydrates, particularly starch, making them a significant energy source[2]. Moreover, chestnuts are packed with essential vitamins and minerals, including vitamin C, B vitamins, potassium, iron, and magnesium, which play crucial roles in various physiological functions[3]. Beyond their nutritional value, chestnuts have been traditionally used in various cultures for their medicinal properties. Recent scientific investigations have corroborated some of these traditional claims, revealing the active functional components in chestnuts that contribute to their health-promoting effects [4-6].

Polysaccharides, intricate carbohydrate structures formed from extended monosaccharide chains, are ubiquitously present in nature, identified in a spectrum of organisms ranging from plants to microorganisms. Over recent decades, the biological activities of these polysaccharides have been at the forefront of scientific exploration, shedding light on their roles in diverse health-centric

applications[7,8]. Documented bioactivities of polysaccharides encompass immunomodulation, anti-inflammatory, antioxidant, and antiviral properties[9-12]. Polysaccharides regulate the immune response at multiple levels and are therefore of great therapeutic value, enhancing the body's defense against various pathogens and diseases. Several mechanisms elucidate the immunomodulatory anti-tumor attributes of polysaccharides. For example, polysaccharides can activate the immune system by enhancing the function and proliferation of key immune entities such as macrophages, T lymphocytes, and natural killer cells, enhancing their ability to target tumors. Besides, polysaccharides can coordinate the spread of specific cytokines, which are essential molecules in the immune signaling cascade that prevents tumor expansion. In addition, polysaccharides can recalibrate the tumor environment, making it less conducive to the proliferation of malignant tumors and more receptive to immune-driven interventions[13].

In this study, chestnut polysaccharides were extracted using the hot water extraction technique and further purified through an efficient three-phase partitioning. By establishing a mouse H22 liver cancer model, the effects of polysaccharides on tumor size variations, organ indices, and tumor inhibition rates were assessed. Inhibition mechanism of polysaccharide on tumor cells were evaluated and explored by employing assays for splenic lymphocyte proliferation, evaluations of macrophage phagocytic capabilities, as well as the exploration of the effects of polysaccharides on peripheral blood lymphocyte subgroups. This research paves the way for elevating the utilization of chestnuts in both medicinal and functional food domains, providing a theoretical foundation for future product research and innovation.

2. Materials and Methods

2.1 Experimental Material

In this investigation, Yanshan chestnuts from Qinglong County, Qinhuangdao, Hebei Province, China were employed as source material. After de-shelling and drying, the kernels were ground and sieved through a 40-mesh screen. The resultant powder was preserved at -20 ℃ for subsequent use. H22 hepatoma cells were provided by the Shanghai Institute of Biological Sciences, Chinese Academy of Sciences. All the female BALB/c nude mice (weight 20 to 25 gm, 7 to 8 weeks old) were obtained from Shanghai SLAC Laboratory Animal Co.,Ltd. MTT, ConA and LPS were purchased from sigma. The antibodies were acquired from Solarbio (Beijing, China). All other chemical reagents were of analytical grade and were obtained from Shanghai Aladdin Biochemical Technology Co., Ltd.

2.2 Instrument and Equipment

ALPHA 2-4 LD Plus Freeze Dryer, N-1100 Rotary Evaporator, UV-5500 UV-Visible Spectrophotometer, OptiClean1300 Super Clean Platform, Avanti J-15R High-Performance Refrigerated Benchtop Centrifuge, 3111 CO_2 Cell Culture Incubator, Eclipse TE2000-U Inverted Microscope, PowerWave XS2 Full-Wavelength Microplate Reader, BD LSRFortessa Flow Cytometer.

2.3 Experimental Method

2.3.1. Extraction and Purification of Chestnut Polysaccharides

50 g of chestnut kernel powder is combined with deionized water at a ratio of 1:20 and stirred for 2 h at 80 ℃. The mixture is then centrifuged at 6000 rpm for 5 min, and the supernatant is collected.

The residue undergoes a second extraction under identical conditions, and the supernatants are combined. The extract is then reduced in volume to 300 mL under vacuum and 60 g of $(NH_4)_2SO_4$ is added. After thorough dissolution through agitation, 450 mL of tert-butanol are added, and the mixture is stirred in a 35 ℃ water bath for 30 min to form a triphasic solution. The solution is then centrifuged at 4000 rpm for 10 minutes to precipitate the proteins. The lower phase is collected and dialyzed for 48 h in a 3000 Da dialysis bag, with deionized water replaced every 12 h. After dialysis, the solution is concentrated and freeze-dried to yield desired chestnut polysaccharides, named as TCP.

2.3.2. Animals Experimental Design

Under aseptic condition, 40 mice were inoculated axillary with 0.2 mL H22 cell suspension (2×10^6 cells/mouse) to establish the liver cancer model. 24 h after the tumor inoculation, the mice were randomly divided into four groups: model group, 5-fluorouracil (5-FU) group, low-dose TCP group, and high-dose TCP group, with 10 mice in each group. In the 5-FU group, 20 mg/(kg d) of 5-FU was given intragastrically to the mice as control group. In contrast, the high-dose group received 500 mg/(kg d) of TCP and the low-dose group 100 mg/(kg d), calculated based on body mass. The mice in the model group were given the same volume of physiologic saline instead of the test solution. All these treatments were administered intragastrically one time daily for 14 days.

2.3.3. Tumor Inhibition Rate and Immune Organ Index

During the experimental period, mice were weighed every two days. Tumor progression was monitored daily once the tumors became palpable or visible. After the last gavage for 12 h, blood sample was collected from the eye socket venous plexus of non-fasting mice. The mice were euthanized by cervical dislocation, then the spleen, thymus, and tumors were excised for the calculation of spleen index, thymus index, and tumor inhibition rate. The organ indexes of spleen and thymus were calculated: organ index (%) = average weight of organ / (average body weight) × 100%. The tumor inhibition rate was calculated as follows: inhibitory rate = (the tumor weight of the model group − the tumor weight of the treatment group) / the tumor weight of the model group × 100%.

2.3.4. Splenocyte Proliferation Assay in Mice

The impact of TCP on mouse splenocyte proliferation was assessed utilizing the MTT assay. Splenocytes from each mouse group were allocated into a 96-well flat-bottom plate, with each well containing 100 μL at a concentration of 1×10^7 cells/mL. The cells were then treated with ConA (5 μg/mL), LPS (10 μg/mL), or RPMI 1640 medium, resulting in a total volume of 200 μL per well. After a 44 h incubation period, the cell density was ascertained by adding 20 μL of MTT solution (5 mg/ml) to each well and measuring the absorbance at 570 nm wavelength. The Stimulation Index (*SI*) was derived using the formula: *SI* = absorbance of cultures with mitogens or TCP / the absorbance of cultures without either.

2.3.5. Macrophage Phagocytosis Assay in Mice

Macrophages (100 μL at 5×10^6 cells/ml) were dispensed into a 96-well flat-bottom plate and incubated for a duration of 3 h. The supernatant was then removed, and each well was treated with 50 μL of 0.073% neutral red. After an additional 30 min incubation, the absorbance of the ingested neutral red was recorded at a wavelength of 540 nm.

2.3.6. Analysis of Lymphocyte Subtypes in Peripheral Blood

Following the euthanization of the mice, lymphocytes were isolated from the peripheral blood after the red blood cells were removed. A sample of 1×10^6 cells was treated with either isotype controls or specific monoclonal antibodies against $CD3^+$, $CD4^+$, $CD8^+$, or $CD19^+$ and incubated for 30 min on ice in darkness. The levels of peripheral blood lymphocyte subgroups in mice were determined by flow cytometry (FCM).

2.3.7. Statistical Analysis

All values were expressed as means ± SD and were analyzed using SPSS 13.0. Differences between groups were assessed by one-way ANOVA and LSD test. A *p*-value of less than 0.05 was considered statistically significant.

3. Results and Analysis

3.1 Effect of TCP on the Change of Tumor Size in H22 Tumor-Bearing Mice

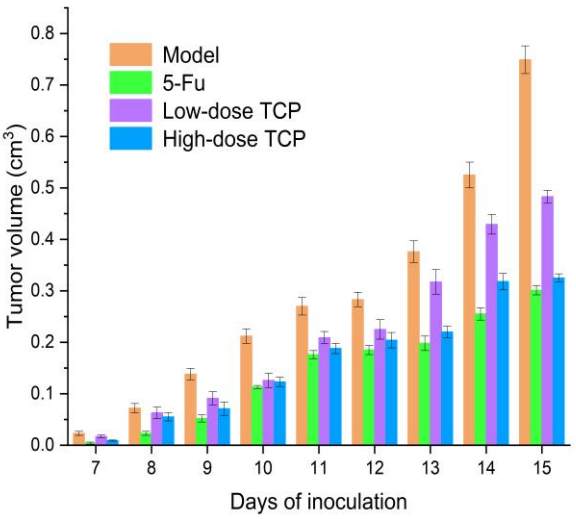

Figure 1: Tumor size changes in H22-bearing mice.

On 7 d post-inoculation with H22 tumor cells, palpable tumors appeared in some mice in the model and polysaccharide groups, and changes in tumor size over time were observed during the experimental period, as illustrated in Figure 1. As the number of post-inoculation days increased, a substantial rise in tumor volume was noted in the model group. The positive control group exhibited the most effective inhibition on the proliferation of H22 tumor cells. Although an upward trend was also observed in the tumor volumes of mice in both dosage groups, the increase was gradual, indicating the inhibitory effect of TCP on the tumors. Both high and low doses of TCP significantly inhibited the growth of tumors in H22 tumor-bearing mice, with the high dose exhibiting superior efficacy. At the end of the experimental period, the average tumor volume in the high-dose group was significantly lower than that in the model group ($p < 0.05$).

3.2 Effect of TCP on Immune Organs of H22 Tumor-Bearing Mice

Table 1: Effect of TCP on organ indexes and tumor inhibition rate in H22-bearing mice (x ± s, n = 10).

Group	Spleen index (mg/g)	Thymus index (mg/g)	Inhibition rate (%)
Model	8.17 ± 0.55#	2.11 ± 0.19#	-
5-Fu	4.10 ± 0.32	3.19 ± 0.27	59.81 ± 2.87
Low-dose TCP	6.16 ± 0.46*	2.45 ± 0.23*	35.64 ± 3.14
High-dose TCP	5.72 ± 0.38*	3.08 ± 0.29*	56.61 ± 2.69

# $p < 0.05$ as compared with the control group. * $p < 0.05$ as compared with the model group.

Following the termination of the experimental stage, mice were dissected, then the thymus, spleen, and tumors of each group were weighed. The spleen and thymus indices of each experimental group were calculated, and the tumor inhibition rates of positive control and TCP dosage groups were derived, as shown in Table 1. Mice in the model group exhibited a marked enlargement of the spleen ($p < 0.05$) and a notable shrinkage of the thymus ($p < 0.05$) compared to the control group. Besides, mice treated with TCP displayed significant variations in spleen and thymus indices compared to the model group ($p < 0.05$). These findings indicate that the immune function of mice in the model group was compromised due to the assault of tumor cells. TCP, while effectively inhibiting tumor growth, managed to maintain the stability of the organ indices in tumor-bearing mice to some extent, thereby safeguarding the immune organs. Additionally, through the dissection and weighing of tumors, the inhibition rates for low and high TCP dosage groups were found to be 35.64% and 56.61%, respectively. The inhibition rate of high-dose TCP group approached that of the positive control group (59.81%), underscoring the capacity of TCP to exert significant control over H22 tumor proliferation.

3.3. Effect of TCP on Lymphocyte Proliferation in H22 Tumor-Bearing Mice

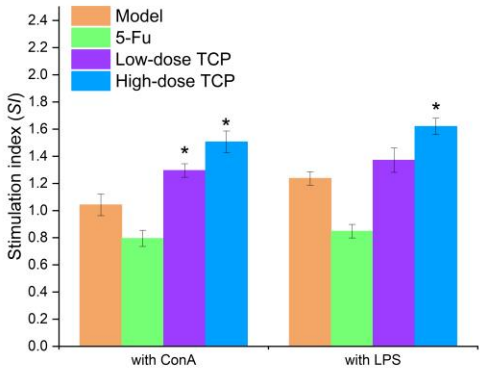

Figure 2: Effect of TCP on the proliferation of spleen lymphocytes from H22 tumor-bearing mice (x ± s, n = 10, * p < 0.05 as compared with the model group)

The proliferation of splenic lymphocytes is a pivotal process in the activation of both cell-mediated and humoral immune pathways, with T-cells and B-cells orchestrating these respective responses. The immunopotentiating efficacy of TCP was assessed by examining the impact on the proliferation of these lymphocytes, stimulated by Concanavalin A (ConA) for T-cells and lipopolysaccharide (LPS) for B-cells. As depicted in Figure 2, TCP significantly augmented both ConA and LPS-induced lymphocyte proliferations in a dose-responsive manner compared to the model group ($p < 0.05$). These findings highlight the significant co-mitogenic property of TCP,

evidencing its role in enhancing the expansion of T and B lymphocytes, modulating cellular and humoral immunities, and consequently culminating in an augmented immune response in tumor-bearing mice.

3.4. Effect of TCP on Macrophage Phagocytosis in H22 Tumor-Bearing Mice

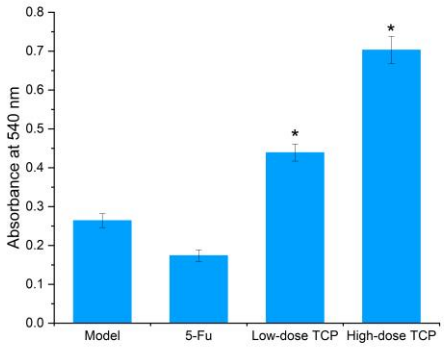

Figure 3: Effect of TCP on macrophage phagocytosis in H22 tumor-bearing mice ($\bar{x} \pm s$, n = 10, * p < 0.05 as compared with the model group)

Macrophage phagocytosis is integral to nonspecific immunity. Extensive research indicates that macrophages are pivotal in initiating innate immune defenses and act as effector cells instrumental in mitigating various responses, including infection, inflammation, angiogenesis, and promoting wound healing. In this study, the macrophage activity in mice was assessed by measuring their phagocytosis of neutral red. Figure 3 illustrates a significant enhancement in macrophage phagocytosis in TCP-treated mice relative to the model group ($p < 0.05$). This indicates that TCP significantly enhances the activity of peritoneal macrophages in tumor-bearing mice, elevating the overall immune response of the organism.

3.5. Effect of TCP on Lymphocyte Subsets in Peripheral Blood

Table 2: Effect of TCP on lymphocyte subsets in peripheral blood in tumor-bearing mice ($\bar{x} \pm s$, n = 10).

Group	$CD3^+$ cells/%	$CD19^+$ cells/%	$CD4^+$ cells/%	$CD8^+$ cells/%
Model	$41.43 \pm 1.21^{\#}$	$50.89 \pm 2.05^{\#}$	$28.46 \pm 1.50^{\#}$	$16.71 \pm 1.25^{\#}$
5-Fu	$60.60 \pm 2.10^{*}$	$35.07 \pm 2.02^{*}$	$33.58 \pm 2.31^{*}$	$21.34 \pm 1.72^{*}$
Low-dose TCP	$54.33 \pm 2.23^{*}$	$45.52 \pm 1.84^{*}$	$32.68 \pm 1.41^{*}$	$19.40 \pm 1.30^{*}$
High-dose TCP	$66.57 \pm 2.45^{*}$	$32.39 \pm 1.39^{*}$	$38.80 \pm 1.47^{*}$	$25.66 \pm 1.94^{*}$

# $p < 0.05$ as compared with the control group. * $p < 0.05$ as compared with the model group.

The ratios of lymphocyte subsets were examined in the peripheral blood of mice bearing H22 tumors, with the data presented in Table 2. There was a notable reduction in the percentages of T cells ($CD3^+$, $CD4^+$, and $CD8^+$) and an elevation in B cells ($CD19^+$) levels in the model group compared to the control group ($p < 0.05$). Mice treated with 5-Fu exhibited a more balanced lymphocyte subset distribution, indicating that 5-Fu exerted a comparable level of toxicity to both T cells and B cells, as evidenced by the reduced lymphocyte counts. In contrast, mice in the TCP group displayed a significant augmentation in T cell proportions ($p < 0.05$) in a dose-responsive manner when compared to the model group. The findings indicated that the mice in the model group were infected as a result of the aggressive growth of H22 hepatoma cells, which aligned with the increased percentage of $CD19^+$ B cells. TCP demonstrated a significant ability to boost the

immune regulation function of $CD4^+$ T cells and enhance the cytotoxic impact of $CD8^+$ T cells, ultimately resulting in the suppression of H22 solid tumor growth.

4. Conclusions

In this experiment, chestnut polysaccharides extracted via hot water and purified using a tri-phase method were tested for its in *vivo* anti-tumor effects against mouse H22 hepatoma cells. Oral administration of TCP to tumor-bearing mice demonstrated a significant inhibitory effect on solid tumors induced by H22 hepatoma cells. Measurement of tumor size revealed that TCP markedly suppressed its growth in mice and alleviated spleen enlargement and thymus atrophy caused by the tumor, thereby enhancing immune function. Additionally, TCP significantly enhanced the proliferation ability of spleen T and B lymphocytes in tumor-bearing mice and improved the phagocytic capacity of peritoneal macrophages. TCP also facilitated the growth of $CD3^+$, CD4+, and $CD8^+$ T lymphocytes, leading to a cytotoxic response against the tumor cells. Thus, TCP exhibits a potent inhibitory effect on H22 transplanted tumors in mice, achieving tumor suppression by indirectly enhancing the immune levels of tumor-bearing mice. Our research has confirmed that TCP is a polysaccharide that exhibits anti-tumor activity by enhancing the host's immune defense mechanisms, offering formidable potential value in the fields of medicine and functional foods.

Acknowledgements

This work was supported by the Project of Hebei Provincial Central Government Guides Local Science and Technology Development (206Z2801G).

References

[1] Yang, F., Huang, X., Zhang, C., Zhang, M., Huang, C. and Yang, H. (2018) Amino acid composition and nutritional value evaluation of Chinese chestnut (Castanea mollissima Blume) and its protein subunit. RSC Advances 8(5), 2653-2659.

[2] Li, R., Sharma, A.K., Zhu, J., Zheng, B., Xiao, G. and Chen, L. (2022) Nutritional biology of chestnuts: A perspective review. Food Chemistry 395, 133575.

[3] Zhang, S., Wang, L., Fu, Y. and Jiang, J.-C. (2022) Bioactive constituents, nutritional benefits and woody food applications of Castanea mollissima: A comprehensive review. Food Chemistry 393, 133380.

[4] Xu, Z., Meenu, M., Chen, P. and Xu, B. (2020) Comparative study on phytochemical profiles and antioxidant capacities of chestnuts produced in different geographic area in China. Antioxidants 9(3), 190.

[5] Liu, C., Wang, S., Chang, X. and Wang, S. (2015) Structural and functional properties of starches from Chinese chestnuts. Food Hydrocolloids 43, 568-576.

[6] Otles, S. and Selek, I. (2012) Effect of processing on the phenolic content and antioxidant activity of chestnuts. Quality Assurance and Safety of Crops & Foods 4(5), e3-e11.

[7] Chen, F. and Huang, G. (2018) Preparation and immunological activity of polysaccharides and their derivatives. International Journal of Biological Macromolecules 112, 211-216.

[8] Mu, S., Yang, W. and Huang, G. (2021) Antioxidant activities and mechanisms of polysaccharides. Chemical Biology & Drug Design 97(3), 628-632.

[9] Xu, H.-S., Wu, Y.-W., Xu, S.-F., Sun, H.-X., Chen, F.-Y. and Yao, L. (2009) Antitumor and immunomodulatory activity of polysaccharides from the roots of Actinidia eriantha. Journal of Ethnopharmacology 125(2), 310-317.

[10] Zhang, Y., Pan, X., Ran, S. and Wang, K. (2019) Purification, structural elucidation and anti-inflammatory activity in vitro of polysaccharides from Smilax china L. International Journal of Biological Macromolecules 139, 233-243.

[11] Yan, J., Zhu, L., Qu, Y., Qu, X., Mu, M., Zhang, M., Muneer, G., Zhou, Y. and Sun, L. (2019) Analyses of active antioxidant polysaccharides from four edible mushrooms. International Journal of Biological Macromolecules 123, 945-956.

[12] Guo, Y., Chen, X. and Gong, P. (2021) Classification, structure and mechanism of antiviral polysaccharides derived from edible and medicinal fungus. International Journal of Biological Macromolecules 183, 1753-1773.

[13] Ying, Y. and Hao, W. (2023) Immunomodulatory function and anti-tumor mechanism of natural polysaccharides: A review. Frontiers in Immunology 14.